Aspects of Coagulation During Emulsion Polymerization of Styrene and Vinyl Acetate

M. F. KEMMERE,[1] J. MEULDIJK,[1] A. A. H. DRINKENBURG,[1] A. L. GERMAN[2]

[1] Laboratory of Chemical Reactor Engineering and Process Development

[2] Department of Polymer Chemistry and Technology, Eindhoven University of Technology, P.O. Box 513, 5600 MB Eindhoven, The Netherlands

Received 13 October 1997; accepted 17 February 1998

ABSTRACT: The influence of recipe and process conditions on the coagulation behavior of polystyrene (PS) and polyvinyl acetate (PVAc) latices has been studied. Seeded batch experiments reveal a significant influence of electrolyte concentration on the coagulation behavior of both PS and PVAc latices. Within the experimental error, no dependency of the coagulation behavior on process conditions, in terms of energy dissipation, reactor scale, impeller type, and impeller diameter, has been observed for the reactor scales investigated. These results indicate that intrinsic chemical influences such as electrolyte concentration dominate the coagulation behavior during emulsion polymerization and also in the absence of polymerization over the process conditions.
 J Appl Polym Sci 69: 2409–2421, 1998

Key words: emulsion polymerization; coagulation; styrene; vinyl acetate; energy dissipation

INTRODUCTION

The product of an emulsion polymerization is a dispersion of submicron polymer particles in a continuous aqueous phase. The rheological properties of the latex depend on the solids content and the particle size (distribution). The particle size (distribution) is among others influenced by coagulation during the stage of particle growth due to absorption of monomer and reaction. Coagulation is caused by a loss of colloidal stability of the latex particles. In commercial processes coagulation may result in off-spec products as well as in troublesome operation. It is, therefore, important to control the particle size of the final product as well as during the polymerization. This article presents an experimental study of the influence of recipe and process conditions on the coagulation behavior of PS and PVAc latices.

COAGULATION IN EMULSION POLYMERIZATION

The colloidal stability of the polymer particles in a latex is mainly governed by electrostatic repulsion when ionic surfactants are used. Coagulation will occur if the kinetic energy of the particles is sufficiently high to overcome the potential energy barrier, being the sum of the Van der Waals attraction energy and the electrostatic repulsion energy. Destabilization may be accelerated by reducing the height of the potential energy barrier (intrinsic chemical influences) as well as by increasing the average kinetic energy of the particles (physical influences).

Correspondence to: J. Meuldijk.
Contract grant sponsor: The Foundation of Emulsion Polymerization (SEP).

Journal of Applied Polymer Science, Vol. 69, 2409–2421 (1998)
 CCC 0021-8995/98/122409-13

Intrinsic Chemical Influences

The recipe used in emulsion polymerization influences the colloidal stability of the polymer particles. Emulsifier occupies the particle surface. A high emulsifier concentration increases the surface charge, resulting in a high electrostatic repulsion. Neighboring particles observe a high energy barrier to coagulate. Colloidal stability is ensured when the fractional surface coverage of the growing particle with emulsifier remains above a critical value (θ_{crit}).[1,2]

Every emulsion polymerization recipe contains some electrolyte originating from the initiator, emulsifier, and pH buffer. Industrial recipes often contain a lot of additives, which may increase the electrolyte concentration even more. A high electrolyte concentration results in a lower energy barrier for approaching particles to coagulate.

Physical Influences

Two mechanisms play a role for physical influences on the coagulation rate of submicron polymer particles: Brownian and shear coagulation. Particles smaller than the Kolmogorov microscale for isotropic turbulence exhibit no inertial effects.[3] The effect of surface coagulation is minimized by controlling the gas–liquid surface area.

Brownian or perikinetic coagulation is related to the Brownian motion of the polymer particles in the latex. The intensity of the Brownian motion is directly proportional to the temperature and inversely proportional to the particle diameter. For similar-sized particles Von Smoluchowski[4] has shown that the rate of Brownian coagulation is governed by a second-order rate equation:

$$J_{Br} = \frac{4k_B T}{3\eta W_{Br}} N_t^2 \qquad (1)$$

where η, W_{Br}, and N_t respectively stand for the dynamic viscosity, the Brownian stability coefficient, and the number of particles per unit volume.

Shear or orthokinetic coagulation is due to the motion of the surrounding liquid. Agitation increases the force as well as the frequency of the collisions between polymer particles. For monodispersed particles smaller than the Kolmogorov microscale the rate of coagulation may be approximated by:

$$J_{Sh} = C_{Sh}\left(\frac{\varepsilon\rho}{\eta}\right)^{0.5} \frac{d_p^3}{W_{Sh}} N_t^2 \qquad (2)$$

where C_{Sh}, ε, ρ, d_p, and W_{Sh} respectively stand for the coagulation coefficient, energy dissipation, density, particle diameter, and shear stability coefficient. In the literature different values are reported for the coagulation coefficient.[5–9]

From eqs. (1) and (2) comes the ratio of the and shear Brownian coagulation:

$$\frac{J_{Sh}}{J_{Br}} = \frac{4W_{Br}d_p^3(\varepsilon\rho\eta)^{0.5}}{3C_{Sh}W_{Sh}k_bT} \qquad (3)$$

If hydrodynamic forces are neglected and W_{Br} equals W_{Sh}, it follows from eq. (3) that the Brownian coagulation dominates over the shear coagulation for submicron particles. In latex systems, however, hydrodynamic and colloidal forces modify the trajectories of the colliding particles ($W_{Br} \neq W_{Sh}$).[10] W_{Sh} decreases with increasing shear rate, whereas W_{Br} is independent of the shear rate.

The power transferred into the mixture, due to stirring, is an important factor for the shear rate in the reactor. Reactor configuration, scale of operation, impeller speed, and impeller type determine the power input. The mean energy dissipation, the power input per unit of mass, is given by:

$$\varepsilon_{av} = \frac{P}{\rho V_R} = \frac{N_p n^3 d^5}{V_R} \qquad (4)$$

where P, V_R, N_p, n, and d, respectively stand for the power input, volume of reaction mixture, power number, impeller speed, and impeller diameter. In the turbulent flow regime, the dimensionless power number is determined by the impeller type and the geometrical arrangement.[11] The energy dissipation distribution in the reactor has been determined for a Rushton turbine impeller using a hot film anemometer[12] and laser doppler velocimetry (LDV).[13,15] Although the absolute values of the energy dissipation vary, these articles all indicate large variations of local energy dissipation between impeller and circulation zone of the tank.

In our laboratory preliminary results of local energy dissipation were determined from LDV measurements in vessels of different size but with equal Rushton geometry.[15] Internal vessel diame-

Table I Dependency of the Rate of Shear Coagulation and Circulation Time on Impeller Diameter, Type, and Speed as Well as Reactor Scale for a Rushton Configuration

Parameter	I	II	J_{ShI}/J_{ShII}	t_{cI}/t_{cII}
Impeller diameter (m)	1/2 D	1/3 D	2.8	0.29
Impeller type	turbine $N_p = 6.3$, $N_c = 2.3$	pitched blade $N_p = 1.4$, $N_c = 1.4$	2.1	0.61
Impeller speed (1/s)	15.0	8.33	2.4	0.56
Reactor scale (dm^3)	0.935	1.85	1.4	0.51

ters ranged from 0.2 to 0.8 m, and the power input was 1 W/kg. These experiments revealed that the energy dissipation distribution is similar for different reactor scales at equal mean energy dissipation.

The circulation time of the liquid back to the impeller region might be important for shear coagulation when there is coagulation and break up in different areas. The circulation time is defined as follows[16]:

$$t_c = \frac{V_R}{N_c d^3 n} \tag{5}$$

where N_c is the circulation number that is a product of the pump number and the circulation ratio. Table I shows the dependency of the shear coagulation rate and circulation time on the process conditions.

EXPERIMENTAL

Batch emulsion polymerization experiments as well as swelling experiments were performed in three baffled stainless steel reactors of different scale (0.935, 1.85, and 7.48 dm^3), with external jackets for heating and cooling. All three vessels have a standard Rushton configuration, except for the flat bottom and some space above the reaction mixture to allow for foaming. The width of the four baffles is 10% of the vessel diameter. A Rushton six bladed turbine impeller and a 45° pitched downflow six-bladed impeller of one-third and a half of the vessel diameter were used. The clearance of the impeller from the bottom was one-half of the vessel diameter. Figure 1 shows a schematic view of the reactor configuration, as well as the impellers used for this study. Table II gives the dimensions of the equipment. For the different reactor scales the mean energy dissipation was kept constant instead of the impeller speed. On every reactor scale, the stirrer speed was varied so that the mean energy dissipation was between 0.2 and 1.5 W/kg.

The coagulation behavior of two latex systems was studied: using the monomers styrene and vinyl acetate. These differ, among other things, in water solubility of the monomers and in polarity of particle surface. The chemicals used in this study were distilled water, commercially grade styrene, and vinyl acetate, supplied by DSM, sodium dodecyl sulfate (emulsifier), sodium persulfate (initiator), sodium carbonate (pH buffer), and sodium chloride (electrolyte), all laboratory grade and supplied by Merck. The temperature was 50.0 ± 0.5 and 35.0 ± 0.5°C for, respectively, the styrene and vinyl acetate experiments. The pH was 10.5 in all cases.

Polymerization

The coagulation behavior of polystyrene particles was studied during emulsion polymerization. To avoid the complex nucleation period and to keep the initial particle number the same for all the experiments, a well-defined polystyrene seed-latex was used. Before usage the synthesized seed-latex was cleaned by dialysis, using a Lundia Alpha 500™ membrane cell. Inorganic salts originating from the buffer and initiator and part of the emulsifier were removed with demineralized water. Although dialysis is not the best method for removal of electrolyte,[17–20] dialysis with a hollow membrane cell has showed to be an efficient tool for cleaning relatively large amounts (10 dm^3) of seed-latex. The influence of this kind of dialysis on the particle size (distribution) of the seed-latex is negligible.

After dialysis of the seed-latex, the particle surface coverage with emulsifier cannot be calculated anymore from the emulsifier concentration in the recipe, because of the partial removal of the surfactant by dialysis. For proper values of the criti-

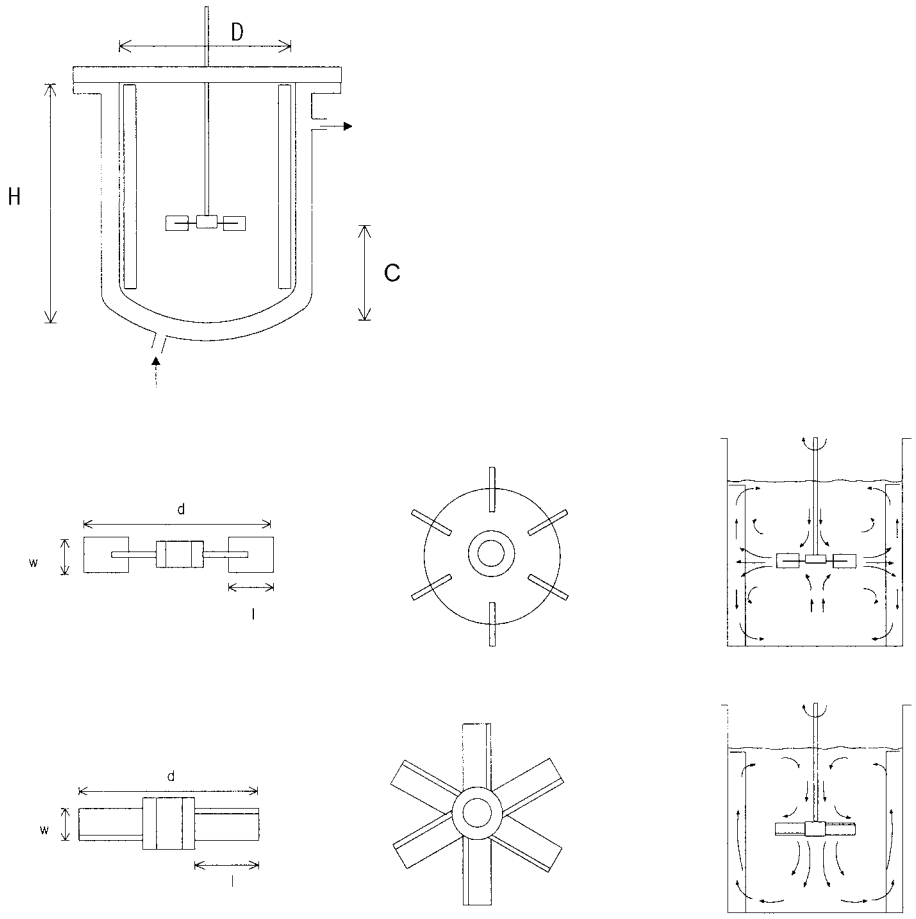

Figure 1 Schematic view of the Rushton polymerization reactors, turbine and 45° pitched six-bladed impellers with corresponding flow patterns.

cal micelle concentration and specific surface area of one emulsifier, the method of Maron[21,22] can be applied to estimate the surface coverage. In Table III the characteristics of the different seed-latices used in this work are given.

Before the start of a polymerization, the reactor was charged with seed-latex, emulsifier, buffer, monomer, and some additional water. For 1 h argon was bubbled through the reaction mixture to remove oxygen. The reaction was started by adding an aqueous initiator solution to the reactor. During the polymerization samples were taken to determine the conversion (by gravimetry) and the volume average particle size using a Jeol 2000 FX Transmission Electron Microscope (TEM).

Swelling Experiment

We performed swelling experiments to study coagulation without polymerization. Because the time scale of limited or controlled particle coagulation is small compared to the time scale of particle growth by polymerization and monomer absorption,[2] it is allowed to study the coagulation behavior of the latex particles as a function of electrolyte concentration without performing emulsion polymerization. The reactor was charged with a seed-latex (for characteristics, see Table III) and monomer, but no initiator was added. In the case of the cleaned polystyrene seed-latices used for the swelling experiments, the lack of sodium ions, originating from the initiator in case of polymerization, has been compensated by adding extra sodium chloride to reach the desirable overall electrolyte concentration. For the polyvinyl acetate swelling experiments, the PVAc seed-latices were not cleaned and diluted before usage, because no polymerization was performed with these seed-latices. Thus, the initial electrolyte concentration was equal to the one used in the recipe of the seed-latex.

Table II Dimensions of the Rushton Polymerization Reactors, Turbine, and 45° Pitched Six-Bladed Impellers

Dimensions of Rushton Polymerization Reactors in (mm)			
Scale (dm^3)	0.935	1.85	7.48
Internal diameter D	106	133	212
Height H	106^+	133^+	212^+
Height impeller C	53	66	106
Diameter baffles d_b	10	13	20
Thickness baffles t_b	1	1.5	2

Dimensions of Six-Bladed Rushton Turbine Impeller in (mm)					
		1.85		7.48	
Scale (dm^3)	0.935 $d = D/3$	$d = D/3$	$d = D/2$	$d = D/3$	$d = D/2$
Impeller diameter d	35	44	66	71	106
Blade width w	7	9	13	14	21
Blade length l	9	11	16	18	26
Blade thickness	1	1.5	1.5	1.5	1.5
Disk diameter	27	33	50	53	79
Disk thickness	1	1.5	1.5	1.5	1.5
Shaft diameter	7	7	7	10	10
Shaft holder diameter	9	12	12	18	27

Dimensions of 45° Pitched Down Flow Six-Bladed Impeller in (mm)				
	1.85		7.48	
Scale (dm^3)	$d = D/3$	$d = D/2$	$d = D/3$	$d = D/2$
Impeller diameter d	44	66	71	106
Blade width w	9	13	14	21
Blade length l	17	25	26	42
Blade thickness	1.5	1.5	1.5	1.5
Shaft diameter	7	7	10	10
Shaft holder diameter	12	12	18	27

The polymer particles were allowed to swell with monomer for 1 h.[23] After the particles were swollen, a sample for particle size analysis was taken every 30 min. After sampling the electrolyte concentration was increased instantaneously. The swelling method is especially suitable to study the

Table III Characteristics of the Polystyrene and Polyvinyl Acetate Seed-Latices Used in This Work

Seed-Latex	PS I	PS II	PVAc I	PVAc II
Final conversion (−)	0.98	0.97	0.97	0.99
Particle size (nm)	40.3	38.0	150	112
Particle number (10^{21} $1/m_w^3$)	9.23	10.8	0.170	0.417
Electrolyte concentration ($kmol/m_w^3$)	0.13	0.12	0.078	0.078
Emulsifier concentration ($kmol/m_w^3$)	0.13	0.12	0.020	0.020
Surface coverage (−)	0.81	0.72	0.34	0.25

coagulation behavior of PVAc-latices because during seeded emulsion polymerization of vinyl acetate homogeneous secondary nucleation occurs. Swelling experiments avoid this problem.

For particle size analysis a Malvern autosizer IIc, based on dynamic light scattering (DLS), and TEM were used. Because polyvinyl acetate has a low glass transition temperature (T_g = 29°C), it is necessary to contrast the particles for TEM analysis. For this purpose several techniques were applied. In literature phosphotungstic acid (PTA)[24,25] as well as uranyl acetate (UAc)[26,27] are mentioned as suitable species for staining polyvinyl acetate particles. From our own experience, staining with 0.5 wt % UAc solution gives better contrast around the particles compared to staining with 2 wt % PTA solution, although in the case of UAc staining the background artifacts are more pronounced than in the case of PTA staining.

RESULTS

The influence of the sodium-ion concentration on the conversion time history and the particle concentration as a function of conversion is shown in Figure 2. The reported sodium concentrations of coagulation experiments include all counter ions in the system, originating from the seed-latex, added salt, initiator, emulsifier, and buffer. The results point to colloidal stability for C_{Na^+} = 0.18 kmol/m_w^3. For higher sodium-ion concentrations, smooth particle coagulation occurs. At an electrolyte concentration of 0.30 kmol/m_w^3 strong, uncontrolled coagulation occurs directly after the start of the seeded reaction. The particle number vs. conversion data, shown in Figure 2(B), sometimes indicate that the particle number at the beginning of the reaction is slightly larger than its initial value. There are two possible explanations for these observations: (1) the experimental accuracy of the particle number is less in the beginning of the experiment than in later stages of the polymerization. The relative large error in particle size and conversion determination in the early stages of the polymerization might mask the results slightly. (2) Some samples are taken only a few minutes after adding the initiator. Start-up effects might occur as well as a little secondary nucleation. After 10 min of polymerization the observed effects have been vanished.

The development of the particle size distribution (PSD) due to particle growth by polymerization and monomer absorption, *and* controlled coagulation during the seeded emulsion polymerization of styrene was studied in detail using TEM (see Fig. 3). The particle number decreases due to coagulation. At an electrolyte concentration of 0.25 kmol/m_w^3 the PSD changes but remains narrow apart from some stochastic broadening. In this case the coagulation process is controlled, the amount of coagulum formed during the polymerization was negligible. The method of collecting scrap, which gives besides the particle number an indication for coagulation, as described by Chern et al. (1996)[28] was, therefore, not applied. The recipe of the experiment depicted in Figure 3 is a good starting point to investigate the influence of process conditions on the coagulation behavior of PS.

The influence of the energy dissipation and reactor scale on the coagulation behavior is presented in Figure 4. The results point to the absence of a significant influence of scale and mean energy dissipation on the conversion time history and the development of the particle number as a function of conversion. During interval II of the polymerization, when the particles grow rapidly due to polymerization and absorption of monomer, the particle number decreases significantly.

The influence of impeller type and diameter is shown in Figure 5. The Rushton turbine impeller generates a radial circulation profile, while a pitched blade impeller gives an axial flow (see Fig. 1). Despite the different macroscopic flow patterns generated by the turbine and pitched blade impeller, the collision frequency of the particles in the smallest eddies and with that the time scale of coagulation is not significantly different for both impellers for the same mean energy dissipation. The results shown in Figure 5 also indicate that within the experimental error an increasing impeller diameter does not increase the coagulation rate, although the circulation time strongly decreases (see Table I).

Swelling experiments have also been used to study the coagulation behavior of PS-latices. The results are similar to those of the polymerization reactions.

In Figures 6 and 7 the results of the swelling experiments with polyvinyl acetate latices are shown. For the experiments shown in Figure 6 a different seed-latex was used as for those presented in Figure 7. Apart from a different starting point, the coagulation behavior is the same. In both Figures 6 and 7 two regions can be distinguished: for $C_{Na^+} \leq 0.2$ kmol/m_w^3 the particle number decreases as a function of the electrolyte

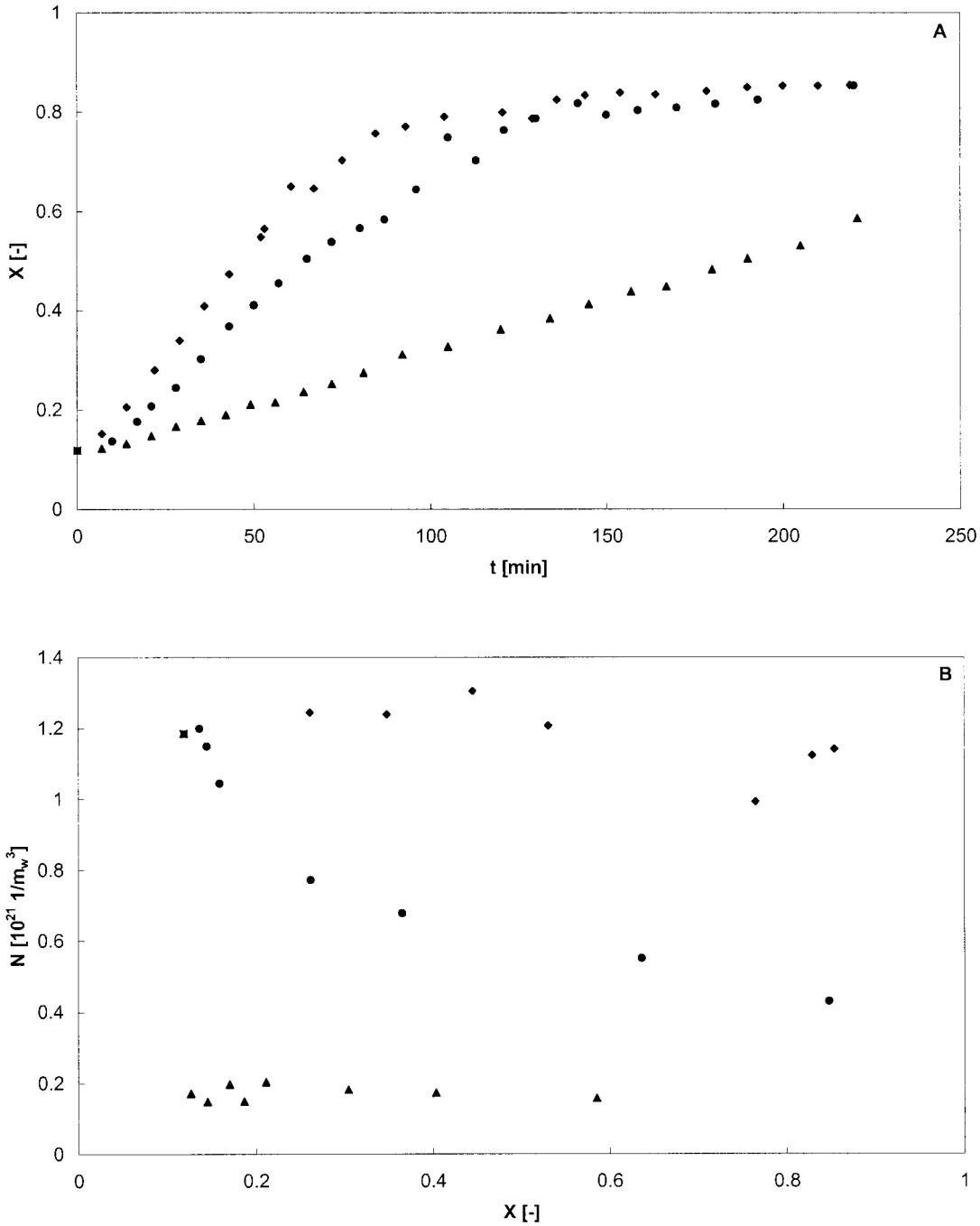

Figure 2 Influence of electrolyte concentration on coagulation behavior of PS-latices during seeded emulsion polymerization on 0.935 dm^3 scale for a Rushton turbine six-bladed impeller with $d = 1/3D$. (A) Conversion time history. (B) Particle number as a function of conversion. Recipe: $C_M = 3.21$ kmol/M_w^3, $C_{SPS} = 0.010$ kmol/m_w^3, $C_{SDS} = 0.016$ kmol/m_w^3, $C_{Na_2CO_3} = 0.0091$ kmol/m_w^3, C_{Na^+}: (♦) 0.18; (●) 0.25; (▲) 0.30 kmol/m_w^3, $N_{p0} = 1.14 \cdot 10^{21}$ 1/m_w^3 (■), seed-latex: PS I, $T = 50.0 \pm 0.5$°C, $\varepsilon_{av} = 0.23$ W/kg.

concentration, whereas for $C_{Na^+} \geq 0.2$ kmol/m_w^3 the particle number is almost independent of the electrolyte concentration. In the first region the electrostatic repulsion between the latex particles decreases due to an increasing electrolyte concentration. In the second region, the electrostatic repulsion no longer contributes to the colloidal stability of the latex system. The only stabilization

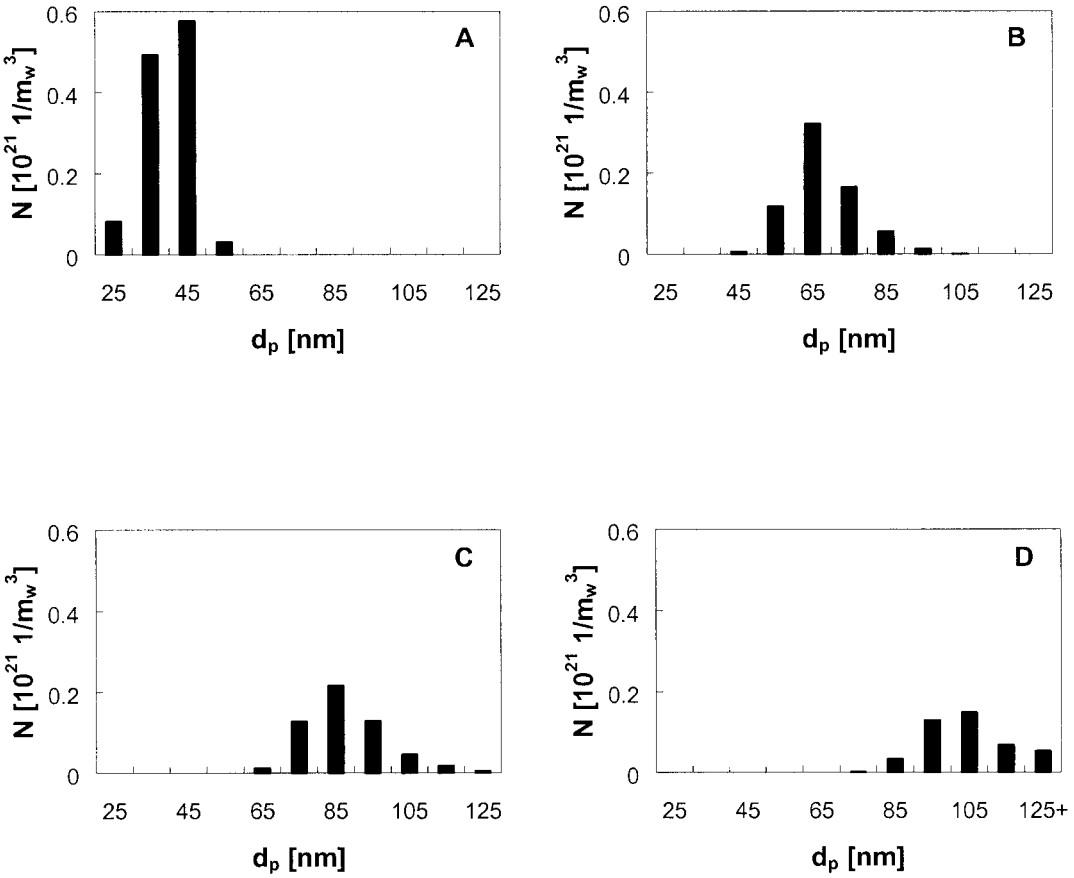

Figure 3 Development of particle size distribution during the seeded emulsion polymerization of styrene determined with TEM on the 0.935 dm^3 scale for a Rushton turbine six-bladed impeller with $d = 1/3D$. Recipe: C_M = 3.21 kmol/m_w^3, C_{SPS} = 0.010 kmol/m_w^3, C_{SDS} = 0.016 kmol/m_w^3, $C_{Na^2CO^3}$ = 0.0091 kmol/m_w^3, C_{Na^+} = 0.25 kmol/m_w^3, $N_{p0} = 1.14 \cdot 10^{21}$ 1/m_w^3 seed-latex: PS I, T = 50.0 ± 0.5°C, ε_{av} = 0.23 W/kg. (A): X = 0.12; (B): X = 0.37; (C): X = 0.64; (D): X = 0.85.

mechanism left is the steric hindrance. As a consequence, there is a resistance for particles for close approach. In agreement with the polystyrene experiments process conditions such as energy dissipation, reactor scale, impeller type, and diameter have no significant influence on the coagulation behavior. When Figure 2 is compared to Figures 6 and 7, the coagulation of PVAc-latices seems to be more sensitive to electrolyte concentration than the coagulation of PS-latices.

DISCUSSION

The effect of agitation during emulsion polymerization has been studied before.[29–32] In agreement with Omi et al.,[32] the emulsion polymerization of styrene is not affected by stirring as long as the emulsification is sufficient. Nomura et al.,[31] however, reported that at higher stirrer speeds, the particle number (determined by TEM analysis) decreases during *ab initio* emulsion polymerization of styrene, while at lower impeller speeds the particle number remains constant. Lowry et al.[30] observed an increase in coagulum formation with impeller speed for an industrial 35 wt % solids latex. These authors did not determine particle numbers during the polymerization itself. Lowry et al.[29] concluded that for the high solids (up to 50 wt %) latices used in their study, shear coagulation was dominating over Brownian. The differences in results are, among others, explained by *ab initio* vs. seeded operation, varying solids content, colloidal stability and the type of latex system, determination of coagulum formation vs. detailed study of particle number by TEM-analysis, etc.

Several authors reported about coagulation of

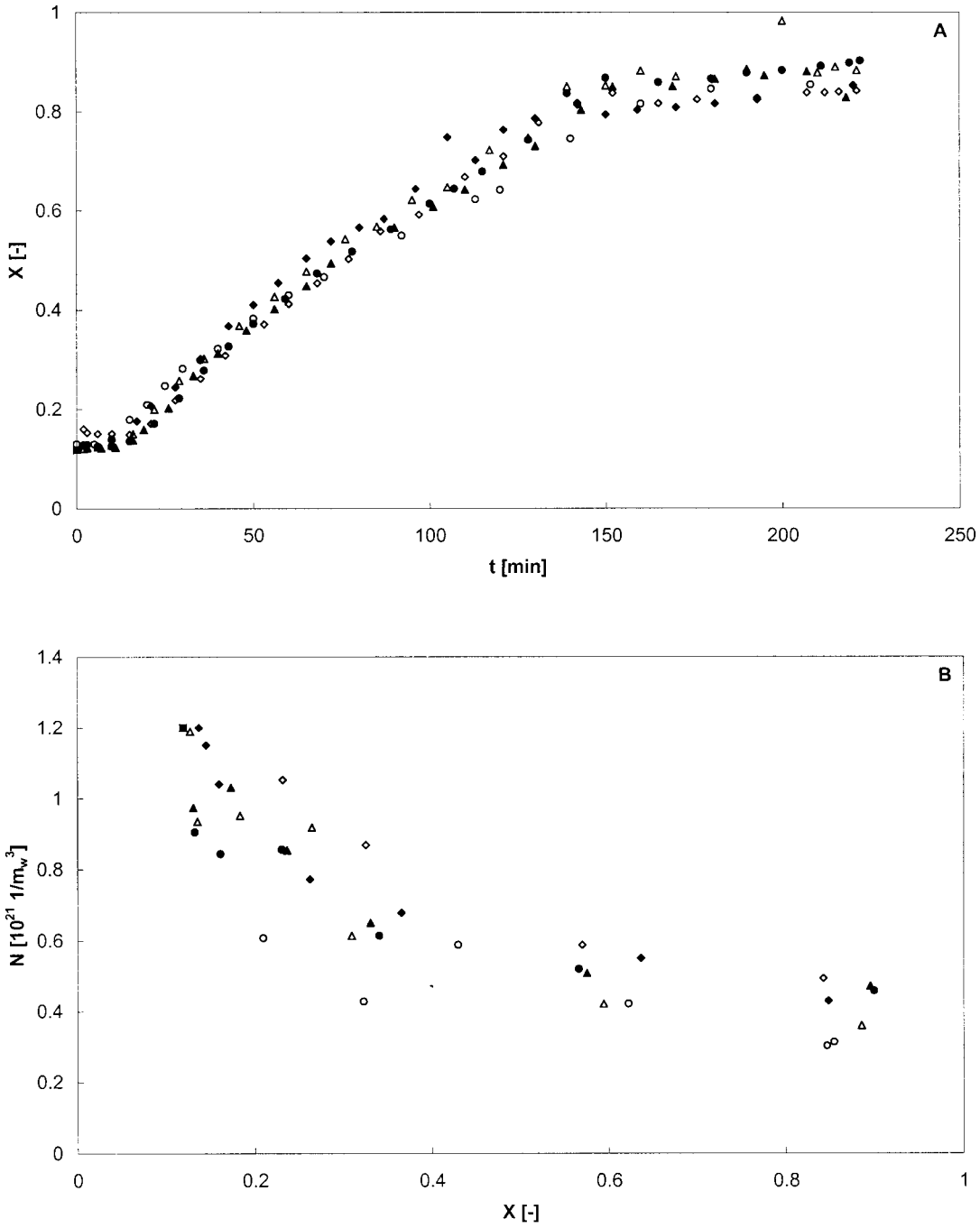

Figure 4 Influence of mean energy dissipation on the coagulation behavior of PS-latices during seeded emulsion polymerization on 0.935^{I} and 1.85^{II} dm^3 scale for a Rushton turbine six-bladed impeller with $d = 1/3D$. (A) Conversion time history. (B) Particle number as a function of conversion. Recipe: $C_M = 3.21$ kmol/M_w^3, $C_{SPS} = 0.010$ kmol/m_w^3, $C_{SDS} = 0.016$ kmol/m_w^3, $C_{Na^2CO^3} = 0.0091$ kmol/m_w^3, $C_{Na^+} = 0.25$ kmol/m_w^3, $N_{p0} = 1.14 \cdot 10^{21}$ $1/m_w^3$ (■), seed-latex: PS I, $T = 50.0 \pm 0.5$°C, ε_{av}: ◆ 0.23^{I}; ○ 0.64^{I}; ▲ 1.37^{I}; ✧ 0.23^{II}; ○ 0.64^{II}; △ 1.37^{II} W/kg.

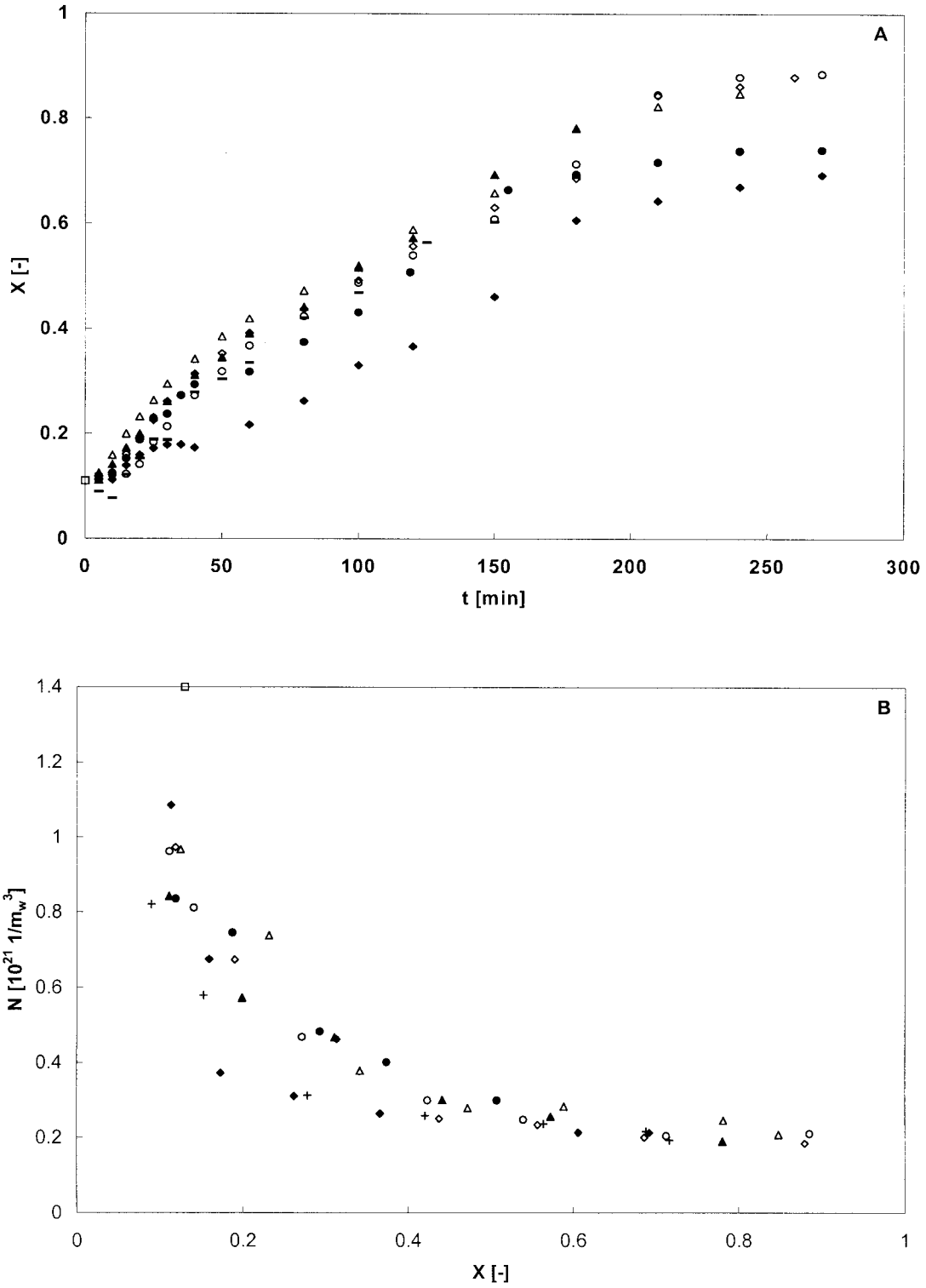

Figure 5 Influence of impeller type and diameter on the coagulation behavior of PS-latices during seeded emulsion polymerization on 1.85^{I} and 7.48^{II} dm^3 scale for turbine (T) and 45° pitched (S) six-bladed impeller. (A) Conversion time history. (B) Particle number as a function of conversion. Recipe: C_M = 3.21 kmol/m_w^3, C_{SPS} = 0.010 kmol/m_w^3, C_{SDS} = 0.016 kmol/m_w^3, $C_{Na^2CO^3}$ = 0.0091 kmol/m_w^3, C_{Na^+} = 0.25 kmol/m_w^3, $N_{p0} = 1.40 \cdot 10^{21}$ 1/m_w^3 (□), seed-latex: PS II, T = 50.0 ± 0.5°C, ε_{av} = 1.54 W/kg, impeller type: ◆ T, $d = 1/3D^{I}$; ● T, $d = 1/2D^{I}$; ■ S, $d = 1/3D^{I}$; ▲ S, $d = 1/2D^{I}$; ✧ T, $d = 1/3D^{II}$; ○ T, $d = 1/2D^{II}$; △ S, $d = 1/2D^{II}$.

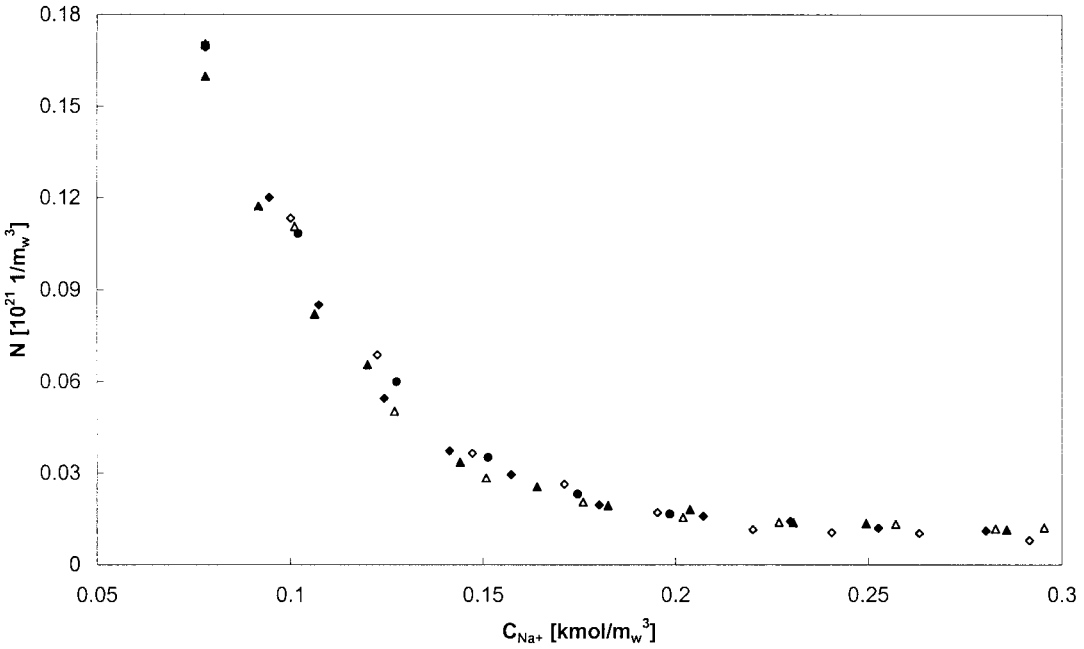

Figure 6 Influence of energy dissipation on the coagulation behavior of PVAc-latices during swelling experiments on 0.935^{I} and 1.85^{II} dm^3 scale for a Rushton turbine six-bladed impeller with $d = 1/3D$. Particle number as a function of electrolyte concentration. Recipe: $C_M = 3.21$ kmol/m_w^3, $C_{SDS} = 0.016$ kmol/m_w^3, $N_{p0} = 0.170 \cdot 10^{21}$ $1/m_w^3$ (■), seed-latex: PVAc I, $T = 35.0 \pm 0.5$°C, ε_{av}: ◆ 0.23^{I}; ● 0.64^{I}; ▲ 1.37^{I}; ✧ 0.23^{II}; ○ 0.64^{II}; △ 1.37^{II} W/kg.

latex systems without reaction.[10,33–35] In agreement with Heller et al.,[34] our PS-latex system starts to coagulate after addition of about 0.20 to 0.25 kmol/m_w^3 electrolyte. Spicer et al.[35] studied the effect of impeller type (Rushton six bladed turbine and 45° pitched four-bladed impeller) and shear rate on floc size and structure during shear induced flocculation of 870 nm PS-particles with $Al_2(SO_4)_3$ as a destabilizing agent. Their results indicate that the steady-state floc size is dependent on the frequency of recirculation to the impeller zone [see eq. (5) and Table I] and the characteristic velocity gradient (influence of impeller type).

The difference from our results is due to the large floc size (>100 μm), the low initial concentration of PS particles, and the use of the strong destabilizing aluminum salt. In their studies on the turbulent coagulation of PS particles of approximately 1 μm, which were considerably larger than those in our experiments, but still smaller than the Kolmogorov microscale, De Boer et al.[33] and Kusters et al.[10] found a dependency on impeller speed. These authors studied low solids systems in which the agglomerates of particles could break up, while during polymerization disrupture of coagulated particles is not probable.

In contrast to several results reported in literature, our study on coagulation indicates that the stage of particle growth (interval II) for 25 wt % solids PS- and PVAc-latices during emulsion polymerization are not determined by the process conditions for reactor scales up to 7.5 dm^3. The coagulation effects in industrial reactors up to 50 m^3 might be different. For instance, we always provided sufficient emulsification in our systems, meaning no creaming of the monomer, which would cause mass transfer limitations. During industrial emulsion polymerization, the emulsification might not be that good, affecting the whole polymerization process, including the coagulation behavior. Besides that, in industry a lot of ingredients are added in a semi-batch operation. If such an addition contains electrolyte originating from, for example, initiator, severe coagulation can occur near the addition point if the mixing of the feed stream with the reactor contents is not fast enough.

CONCLUSIONS

For studying the coagulation behavior of polymer particles during emulsion polymerization it is im-

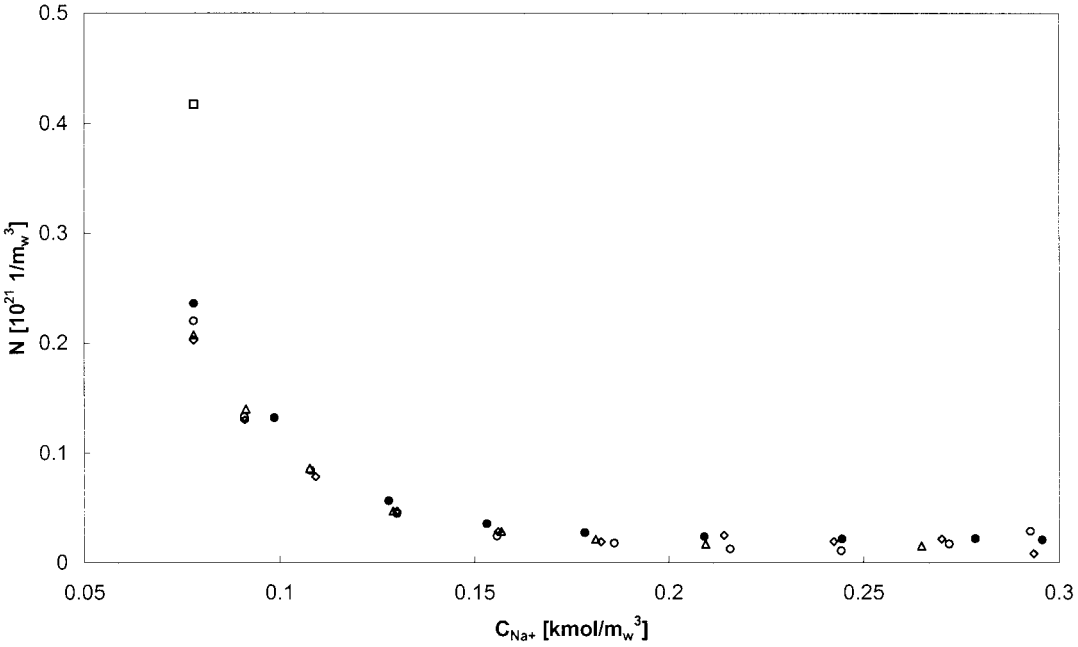

Figure 7 Influence of impeller type and diameter on the coagulation behavior of PVAc-latices during swelling experiments on 1.85 dm^3 scale for turbine (T) and 45° pitched (S) six-bladed impeller. Particle number as a function of electrolyte concentration. Recipe: $C_M = 3.21$ kmol/m_w^3, $C_{SDS} = 0.016$ kmol/m_w^3, $N_{p0} = 0.417 \cdot 10^{21}$ 1/m_w^3 (□), seed-latex: PVAc II, $T = 35.0 \pm 0.5$°C, ε_{av}: 1.37 W/kg, impeller type: ○ T, $d = 1/3D$; ● T, $d = 1/2D$; △ S, $d = 1/3D$; ▲ S, $d = 1/2D$.

portant to perform seeded reactions to exclude effects from the nucleation interval on the development of the particle size distribution.

To avoid secondary nucleation effects in studying the coagulation behavior of polyvinyl acetate latices, swelling experiments are useful. The same effects in coagulation behavior were found during the polymerization experiments.

The electrolyte concentration dominates the coagulation behavior of both PS and PVAc latices over the influence of equipment and operating conditions, expressed in energy dissipation, tank scale, impeller type, and impeller diameter.

The coagulation of PVAc-latices appears to be more sensitive to electrolyte concentration than the coagulation of PS-latices.

In contrast with Nomura et al.[31], Lowry et al.,[29,30] and in agreement with Omi et al.,[32] no influence of impeller speed on the coagulation rate of PS- and PVAc-latices was observed for the reactor scales investigated.

Although changing the impeller type and impeller diameter strongly influences the flow behavior on macroscale, it hardly affects the coagulation behavior of polymer particles within the Kolmogorov microscale of isotropic turbulence for reactor scales up to 7.5 dm^3.

The authors wish to thank the Foundation of Emulsion Polymerization (SEP) for the financial support of this study and the students J. J. G. Coolen, R. J. T. H. Lensing, and L. A. M. Limpens for their contribution to this work. We acknowledge the useful comments by prof. D. Thoenes during the review of our manuscript.

NOMENCLATURE

C	clearance of impeller from tank bottom (m)
Ce_0	emulsifier concentration (kmol/m_w^3)
C_{I0}	initial initiator concentration (kmol/m_w^3)
C_{M0}	initial monomer concentration (kmol/m_w^3)
C_{Na^+}	electrolyte concentration (kmol/m_w^3)
C_{Sh}	coefficient for shear coagulation (−)
d	impeller diameter (m)
D	internal tank diameter (m)
d_p	particle diameter (m)
H	height of reactor (m)
J_{Br}	coagulation rate for Brownian coagulation (1/m_w^3 s)

J_{Sh}	coagulation rate for shear coagulation ($1/m_w^3$ s)
k_B	Boltzmann constant (J/K)
l	impeller blade length (m)
N	particle number ($1/M_w^3$)
n	rotational impeller speed (1/s)
N_0	initial particle number ($1/M_w^3$)
N_p	power number (−)
t	time (s)
t_c	circulation time (s)
T	temperature (°C)
V_R	volume of reaction mixture (m^3)
w	impeller blade width (m)
W_{Br}	stability coefficient for Brownian coagulation (−)
W_{Sh}	stability coefficient for shear coagulation (−)

Greek

η	viscosity (Pa s)
ρ	density ($kg/m^{3)}$)
ε_{av}	average energy dissipation (W/kg)
θ_{crit}	critical surface coverage of the polymer particles with emulsifier below which coagulation occurs (−)

Acronyms

DLS	dynamic light scattering
LDV	laser doppler velocimetry
PS	polystyrene
PSD	particle size distribution
PTA	phosphungstic acid
PVAc	polyvinyl acetate
TEM	transmission electron microscopy
UAc	uranyl acetate

REFERENCES

1. J. Meuldijk, G. F. M. Hoedemakers, M. J. J. Mayer, and D. Thoenes, *Dechema Monogr.,* **127,** 417 (1992).
2. M. J. J. Mayer, J. Meuldijk, and D. Thoenes, *J. Appl. Polym. Sci.,* **56,** 119 (1995).
3. F. E. Kruis and K. A. Kusters, *Chem. Eng. Commun.,* **158,** 201 (1997).
4. M. von Smoluchowski, *Z. Phys. Chem.,* **92,** 129 (1917).
5. T. R. Camp and P. C. Stein, *J. Boston Soc. Civil Eng.,* **30,** 219 (1943).
6. M. A. Delichatsios and R. F. Probstein, *J. Colloid Interface Sci.,* **5,** 394 (1974).
7. K. Higashitani, K. Yamauchi, Y. Matsuno, and G. Hosokawa, *J. Chem. Eng. Jpn.,* **16,** 299 (1983).
8. V. G. Levich, *Physico Chemical Hydrodynamics,* Prentice Hall, Englewood Cliffs, NY, 1962, p. 216.
9. P. G. Saffman and J. S. Turner, *J. Fluid Mech.,* **1,** 16 (1956).
10. K. A. Kusters, J. G. Wijers, and D. Thoenes, *Chem. Eng. Sci.,* **52,** 107 (1997).
11. J. H. Rushton, E. W. Costich, and H. J. Everett, *Chem. Eng. Prog.,* **46,** 9 (1950).
12. Y. Okamoto, M. Nishikawa, and K. Hashimoto, *Int. Chem. Eng.,* **21.** 88 (1981).
13. J. Costes and J. P. Couderc, *Chem. Eng. Sci.,* **43,** 2765 (1988).
14. H. Wu and G. K. Patterson, *Chem. Eng. Sci.,* **44,** 2207 (1989).
15. A. F. Kajbic, graduate report in Process and Product Design, ISBN 90–5282–453–3 (1995).
16. D. Thoenes, Chemical Reactor Development, from laboratory to industrial production, Kluwer Academic Publishers, **64** (1994).
17. J. G. Brodnyan and E. L. Kelley, *J. Coll. Sci.,* **20,** 7 (1964).
18. H. A. Edelhauser, *J. Pol. Sci.,* **27,** 291 (1969).
19. C. G. Force, E. Matijevic, and J. P. Kratchvil, *Koll. Z. Z. Pol.,* **223,** 31 (1967).
20. R. A. Ottewill and J. N. Shaw, *Koll. Z. Z. Pol.,* **215,** 161 (1966).
21. S. H. Maron, M. E. Elder, and I. N. Ulevitch, *J. Col. Sci.,* **9,** 89 (1954).
22. K. J. Abbey, J. R. Erickson, and R. J. Seidewand, *J. Col. Int. Sci.,* **66,** 1 (1978).
23. L. F. J. Noël, R. Q. F. Jansssen, W. J. M. van Well, A. M. van Herk, and A. L. German, *J. Col. Int. Sci.,* **175,** 461 (1995).
24. O. L. Shaffer, M. S. El-Aasser, and J. W. Vanderhoff, 41st Ann. Mtg. Electro. Microscopy Soc. Am., 30 (1983).
25. B. J. Spit, 5th Int. Congress Electron Microscopy, BB-7 (1962).
26. A. M. Hodge and R. C. Bassett, *J. Mat. Sci.,* **12,** 2065 (1977).
27. B. J. Spit, *Faserforschung und Textiltechnik,* **18,** 161 (1967).
28. C. S. Chern, H. Hsu, and F. Y. Lin, *J. Appl. Pol. Sci.,* **60,** 1301 (1996).
29. V. Lowry, M. S. El-Aasser, and J. W. Vanderhoff, *J. Appl. Polym. Sci.,* **29,** 3925 (1984).
30. V. Lowry, M. S. El-Aasser, J. W. Vanderhoff, A. Klein, and C. A. Silebi, *J. Coll. Int. Sci.,* **112,** 521 (1986).
31. M. Nomura, M. Harada, and W. Eguchi, *J. Appl. Polym. Sci.,* **16,** 835 (1972).
32. S. Omi, Y. Shiraishi, H. Sato, and H. Kubota, *J. Chem. Eng. Japan,* **2,** 64 (1969).
33. G. B. J. de Boer, G. F. M. Hoedemakers, and D. Thoenes, *Chem. Eng. Res. Dev.,* **67,** 301 (1989).
34. W. Heller and W. B. de Lauder, *J. Coll. Int. Sci.,* **35,** 60 (1971).
35. P. T. Spicer, W. Keller, and S. E. Pratsinis, *J. Coll. Int. Sci.,* **184,** 112 (1996).